BIOCHEMICAL PHARMACOLOGY 77 (2009) 770–780

available at www.sciencedirect.com

ScienceDirect

journal homepage: www.elsevier.com/locate/biochempharm

Inhibition of CHK1 kinase by Gö6976 converts 8-chloro-adenosine-induced G2/M arrest into S arrest in human myelocytic leukemia K562 cells

Xiu-Zhen Jia [a,1], *Sheng-Yong Yang* [a,b,1], *Jing Zhou* [c], *Shu-Yan Li* [a], *Ju-Hua Ni* [a], *Guo-Shun An* [a], *Hong-Ti Jia* [a,c,*]

[a] *Department of Biochemistry and Molecular Biology, Peking University Health Science Center, Xue Yuan Road 38, Beijing 100191, PR China*
[b] *Molecular Medicine and Cancer Research Center,Chongqing Medical University, Yi Xue Yuan Road 1, Chongqing 400016, PR China*
[c] *Department of Biochemistry and Molecular Biology, Capital Medical University, You An Men 8, Beijing 100054, PR China*

ARTICLE INFO

Article history:
Received 26 September 2008
Accepted 10 November 2008

Keywords:
8-Chloro-adenosine
DNA damage
G2/M checkpoint
Intra-S-phase checkpoint
CHK1 inhibitor/Gö6976
Human myelocytic leukemia K562 cell

ABSTRACT

8-Chloro-cAMP (8-Cl-cAMP) and its metabolite 8-chloro-adenosine (8-Cl-Ado) inhibit cell growth by 8-Cl-Ado-converted 8-Cl-ATP that targets cell-cycle control and RNA metabolism. However, the cell-cycle checkpoint pathways remain to be identified. Recent studies have shown that 8-Cl-cAMP administration and 8-Cl-Ado exposure may damage chromosomal DNA *in vivo* and *in vitro*. In this study, we demonstrate that 8-Cl-Ado-induced DNA damage activates G2/M phase checkpoint, which is associated with ATM-activated CHK1-CDC25C-CDC2 pathway joined by BRCA1-CHK1 branch in apoptosis-resistant human myelocytic leukemia K562 (p53-null) cells. Inhibition of CHK1 kinase by Gö6976, an inhibitor of CHK1 activity, can promote DNA damage and lead to the activation of CHK2, converting G2/M checkpoint into intra-S-phase checkpoint in which two parallel branches, the ATM-CHK2-CDC25A-CDK2 and the ATM-NBS1/SMC1 cascades, are involved. These observations may provide aid in better understanding of the mechanisms of 8-Cl-cAMP and 8-Cl-Ado actions and in potential design of the combined therapy.

1. Introduction

8-Chloro-cyclic-adenosine monophosphate (8-Cl-cAMP) is a potential anti-cancer agent [1–10] that exerts its cytotoxicity by converting into its metabolite, 8-chloro-adenosine (8-Cl-Ado) [6–9]. Cell-cycle arrest and apoptosis are considered to be responsible for this effect. The regulations of protein kinase A [1], protein kinase C [9] and p38 MAP kinase [10] in the inhibitory proliferation of 8-Cl-cAMP- and 8-Cl-Ado-targeted cells have been reported. It shows that in living cell, 8-Cl-Ado can be phosphorylated to the moiety of 8-Cl-ATP [8] that can inhibit RNA synthesis *in vivo* and *in vitro* by chain termination and inhibition of poly(A) polymerase [11,12]. Although selective induction of apoptosis by 8-Cl-cAMP has been observed [3], cytogenetic study shows chromosome cleavage in polychromatic erythrocytes in BALB/c mice administrated with 8-Cl-cAMP [13]. Supporting this observation, we have recently found that 8-Cl-Ado/8-Cl-ATP can induce DNA double-stranded breaks (DSBs) through inhibiting type II topoisomerase (Topo II) activities in human leukemia K562

* *Corresponding author at*: Department of Biochemistry and Molecular Biology, Peking University Health Science Center, Xue Yuan Road 38, Beijing 100191, PR China. Tel.: +86 10 82801434/82801158; fax: +86 10 82801434.
E-mail address: jiahongti@bjmu.edu.cn (H.-T. Jia).

[1] Xiu-Zhen Jia and Sheng-Yong Yang contributed equally to this work.

0006-2952/$ – see front matter © 2008 Elsevier Inc. All rights reserved.
doi:10.1016/j.bcp.2008.11.008

cells [14]. Thus, the molecular mechanisms of 8-Cl-cAMP actions are complicated, in which DNA damage may be involved.

When cells encounter DNA damage, a cascade of signal pathways activates cell-cycle checkpoints, DNA repair and/or apoptosis, which allow cells to limit heritable mutations in daughter cells, maintaining genomic stability [15–17]. These cellular responses are closely correlated with toxicities, tumorigenesis and chemotherapy. ATM (Ataxia telangiectasia mutated) and ATR (ATM and Rad3-related) play critical roles in response to DNA damage. ATM is activated mainly by DNA DSBs. ATR responds to a wider range of signals, including UV-induced damage, DSBs and stalled replication forks [15]. The checkpoint functions of ATM and ATR are mediated partly by the checkpoint effector kinases, CHK2 and CHK1. Activated CHK2 and CHK1 phosphorylate/inactivate the CDC25 family of phosphatases, thereby maintaining CDC2/CDK1 in its phosphorylated inactive form which leads to a G2/M arrest [15–17].

In response to DNA DSBs, ATM phosphorylates histone H2AX on Ser-139 (γ-H2AX), forming nuclear foci specifically at the damaged sites containing DSBs [18]. The formation of γ-H2AX foci can facilitate the recruitment of damage-responsive proteins and chromatin remodeling complexes to the sites of DNA damage, and influence the efficiency and fidelity of DSB repair [18,19]. These recruited proteins include Nijmegen breakage syndrome 1 (NBS1), structural maintenance of chromosomes 1 (SMC1), and breast cancer 1 (BRCA1) which are phosphorylated by ATM/ATR and CHKs in response to DNA damage. ATM phosphorylates/activates NBS1 in the MRE11–RAD50–NBS1 complex and S checkpoint control [15,20]. Also, ATM-activated SMC1 plays a role in S-phase checkpoint [15,21,22]. BRCA1 plays important role in S and/or G2M checkpoint [15,23].

It is believed that abrogation of G2 checkpoint often leads to an increase in the sensitivity of cells to ionizing radiation and chemotherapeutic agents [24]. The CHK1 inhibitor Gö6976, an indolocarbazole with a similar structural backbone to UCN-01 that is originally identified as a protein kinase C inhibitor, can potently inhibit DNA damage-induced S [25] and G2 [25,26] cell-cycle checkpoints, thereby sensitizing tumor cells to DNA-damaging agents [25].

We have previously reported that 8-Cl-Ado induces G2/M arrest in human lung cancer cell line A549 and H1299, in which the targeted cells are able to exit the G2 phase and enter the M phase due to loss of phosphorylated forms of CHK2 and CDC25C, followed by mitotic catastrophe [27]. Also, we have demonstrated that 8-Cl-Ado-induced G2/M arrest and mitotic dividing failure are correlated partly to the disruption of dynamic instability of microtubules and microfilaments [28]. Recently, we found that 8-Cl-Ado exposure can induce DNA DSBs through inhibiting type II topoisomerases by 8-Cl-Ado-converted 8-Cl-ATP in human leukemia K562 cells [14]. In this study, we demonstrate that 8-Cl-Ado exposure activates ATM-CHK1-CDC25C-CDC2 cascade joined by BRCA1-CHK1 branch in the response to 8-Cl-Ado-induced DNA damage, arresting K562 in the G2/M phase. Inhibition of CHK1 by Gö6976 promotes 8-Cl-Ado induced DNA damage and stimulates CHK2 activation, converting G2/M checkpoint into S-phase checkpoint in which the ATM-CHK2-CDC25A-CDK2 and the ATM-NBS1/SMC1 parallel cascades are involved.

2. Materials and methods

2.1. Cell culture and chemical treatment

Human chronic myelocytic leukemia K562 cell (ATCC, Rockville, MD) was cultured in RPMI 1640 medium supplemented with 10% fetal bovine serum (GIBCO BRL, Carlsbad, CA), 100 U/ml penicillin and 100 mg/ml streptomycin, and grown in a 37 °C incubator with 5% CO_2.

8-Cl-Ado (The State Laboratory for Natural and Biomimetic Drugs, Peking University HSC, China) was dissolved in sterilized 0.85% NaCl solution and added to cultures at the concentration of 10 μM for the indicated times. Gö6976 (Calbiochem, La Jolla, CA) (0.1–1.0 μM) was dissolved in 0.1% DMSO solution and added to cultures for 30 min prior to 8-Cl-Ado exposure.

2.2. Immunocytochemical labeling

Immunocytochemical labeling was performed as described [28,29] with modifications. Briefly, cells were fixed with 4% formaldehyde in PBS at 37 °C for 30 min, washed in PBS, and then permeabilized with 0.5% Triton X-100 in PBS for 20 min at room temperature. Cells were washed in a blocking solution consisting of 5% BSA and 0.2% Triton X-100 and stored in the blocking solution at 4 °C till labeling. For labeling, fixed cells were incubated for 2 h at 37 °C with specific antibodies against to phospho-H2AX-S139 (γ-H2AX) (1:2000) (R&D Systems Inc., Minneapolis, MN), phospho-ATM-S1981 (1:1500), phospho-CHK2-T68 (1:1500), CDC45 (1:100), p21 (1:100) (Cell Signaling Technology, Beverly, MA) in the blocking solution, respectively, followed by three washes in blocking solution. Cells were incubated with Rhodamine-conjugated goat anti-rabbit IgG (1:100) or FITC-conjugated goat anti-mouse IgG (1:100) (Santa Cruz Biotechnology Inc., Santa Cruz, CA) in the blocking solution at 37 °C for 1 h. After three washes, cells were incubated for 10 min at room temperature with 5 mg/ml Hoechst 33342 (Molecular Probes, Eugene, OR). After three washes in PBS, cells were mounted in a 90% glycerol–PBS mixture. Laser confocal microscopy was performed at room temperature using Leica TCS SP2 (Leica Microsystems Heidelberg GmbH, Mannheim, Germany).

2.3. Flow cytometry analysis

Cell-cycle analysis was performed as previously described [27]. Aliquots of cells (1.5×10^6) were pelleted and washed twice in cold PBS, and fixed in ice-cold 70% ethanol overnight at 4 °C. Then the cells were washed in PBS and digested with DNase-free RNase A (10 μg/ml) at 37 °C for 30 min. Before flow cytometry analysis, cells were resuspended in 1 ml of propidium iodide (10 μg/ml) (Sigma–Aldrich, St. Louis, MO) for DNA staining. Three independent experiments were performed and cellular DNA contents were analyzed by FACScan (Becton Dickinson, Franklin Lakes, NJ). For cell-cycle analysis, computer programs CELL Quest and ModFit LT 2.0 for Power were used.

2.4. Coimmunoprecipitation studies

Cells were collected by centrifugation, lysed in ice-cold coimmunoprecipitation (co-IP) lysis buffer containing 50 mM

Tris (pH 7.4), 150 mM NaCl, 1% NP-40, 0.25% Na-deoxycholate, 1 mM EDTA, protease inhibitor cocktail (Roche Diagnostics, Mannheim, Germany), and protein phosphatase inhibitor cocktails I and II (EMD Biosciences Inc., La Jolla, CA) and incubated on ice for 10 min. Insoluble material was pelleted at 13,000 × *g* for 10 min at 4 °C. The supernatant was then precleaned by protein A- and protein G-agarose (Roche), and aliquots were coimmunoprecipitated with either nonspecific IgG or specific antibody against to phospho-BRCA1-S1524 (Cell Signaling Technology) in co-IP lysis buffer at 4 °C for 3 h. Protein A-agarose was added, and the mixture was incubated at 4 °C for 2 h. The immunoprecipitated complex was washed with co-IP washing buffer (200 mM Tris [pH 7.4], 150 mM NaCl, 0.5% NP-40, and 1 mM EDTA) five times and with co-IP lysis buffer once. The immunoprecipitate was analyzed by SDS-PAGE.

2.5. *Western blotting*

Cells were lysed in lysis buffer. The proteins of the lysates were quantified with BCA™ Protein Assay Kit (Pierce, Rockford, IL). Fifty micrograms of total proteins were subjected to 6–12% SDS-PAGE and transferred onto nitrocellulose membranes, blocked with 5% nonfat milk in TBS-T (20 mM Tris, 500 mM NaCl, and 0.1% Tween 20) at room temperature for 2 h with rocking. The membranes were probed with specific antibodies overnight at 4 °C. After washing with 5% nonfat milk/TBS-T three times for 15 min each, membranes were incubated with horseradish-peroxidase-conjugated secondary antibodies (Santa Cruz Biotechnology Inc.) in 5% nonfat milk/TBS-T at room temperature for 1 h. After washing three times in TBS-T for 15 min, the protein–antibody complex was detected by enhanced chemiluminescence (Santa Cruz Biotechnology Inc.). Equal protein loading was verified by rehybridization of membranes and reprobed with anti-Actin antibody. Specific antibodies against to CHK1, phospho-CHK1-S345, CHK2, phospho-CHK2-T68, CDC25A, CDC25C, phospho-CDC25C-S216, CDC2, phospho-CDC2-Y15, phospho-BRCA1-S1524, phospho-NBS1-S343, phospho-SMC1-S957, p21Waf1/Cip1, phospho-CDK2-T160, and PARP were from Cell Signaling Technology. Anti-Actin, anti-CDK2, and anti-CDC45 antibodies were from Santa Cruz Biotechnology. Anti-ATM, anti-phospho-ATM-S1981, and anti-γ-H2AX antibodies were from R&D Systems Inc.

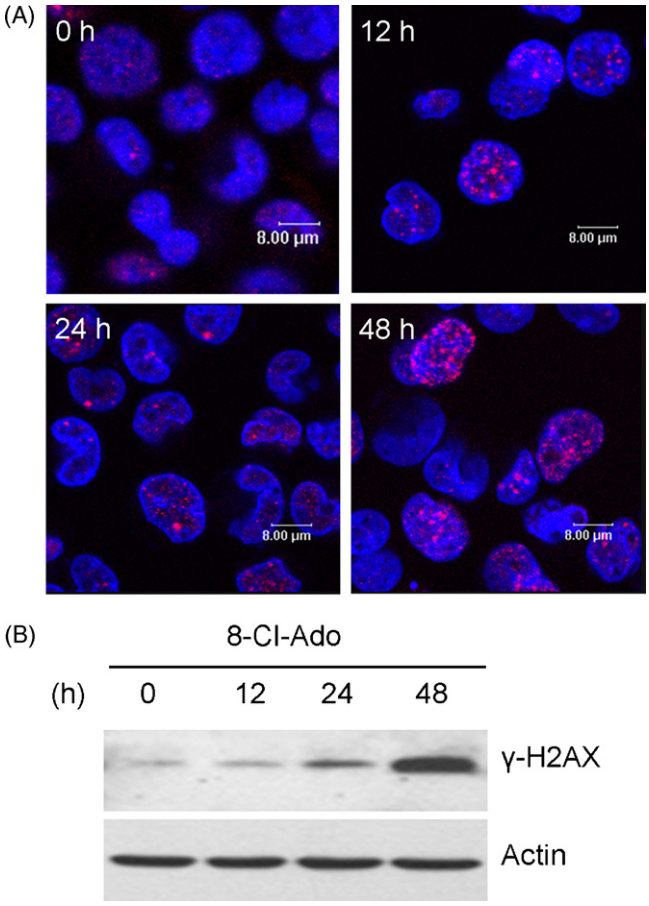

Fig. 1 – Increased H2AX phosphorylation and focalization in 8-Cl-Ado-exposed K562. The cells were exposed to 10 μM 8-Cl-Ado for 0 (unexposed), 12, 24 and 48 h, respectively. (A) Immunofluorescence showing focalization of γ-H2AX. After harvested, the cells were immunolabeled with anti-γ-H2AX antibody and Rhodamine-conjugated goat anti-rabbit secondary antibody (red). The nuclei were stained with Hoechst 33342 (blue). Cells were dropped on slides and viewed with Leica TCS SP2 confocal microscopy. Scale bar, 8 μm. (B) Western blotting showing a time-dependent increase of γ-H2AX. After the cells were extracted with lysis buffer, proteins were separated by 12% SDS-PAGE and transferred onto membrane, the blot was probed with anti-γ-H2AX antibody. β-Actin is used as a loading control.

3. Results

3.1. *8-Cl-Ado exposure induces DNA DSBs in K562 cells*

When cells encounter DSBs, the phospho-H2AX-S139 (γ-H2AX) is generated, forming discrete nuclear foci at the damaged sites [18]. To demonstrate 8-Cl-Ado-induced DSBs, we examined γ-H2AX nuclear foci in exposed K562 cells by immunocytochemical labeling (Fig. 1A). The numbers of γ-H2AX foci were significantly increased within 12–48 h after exposure. Consistent with the increase of γ-H2AX foci, the levels of γ-H2AX protein were globally increased after exposure (Fig. 1B). Increased γ-H2AX was also observed in exposed A549, H1299, HL60 and AT (ATM-deficient) cells (data not shown). These results are consistent with our recent observation of 8-Cl-Ado-induced DNA DSBs in pulsed field gel electrophoresis [14], and indicate that 8-Cl-Ado exposure can induce DNA damage in common.

3.2. *Formation of γ-H2AX is associated with ATM activation*

After DNA damage, ATM molecule in the cell is rapidly autophosphorylated on Ser-1981, and ATM-dependent phosphorylation of histone H2AX on Ser-139 occurs [15,18]. To demonstrate whether the phosphorylation of histone H2AX on

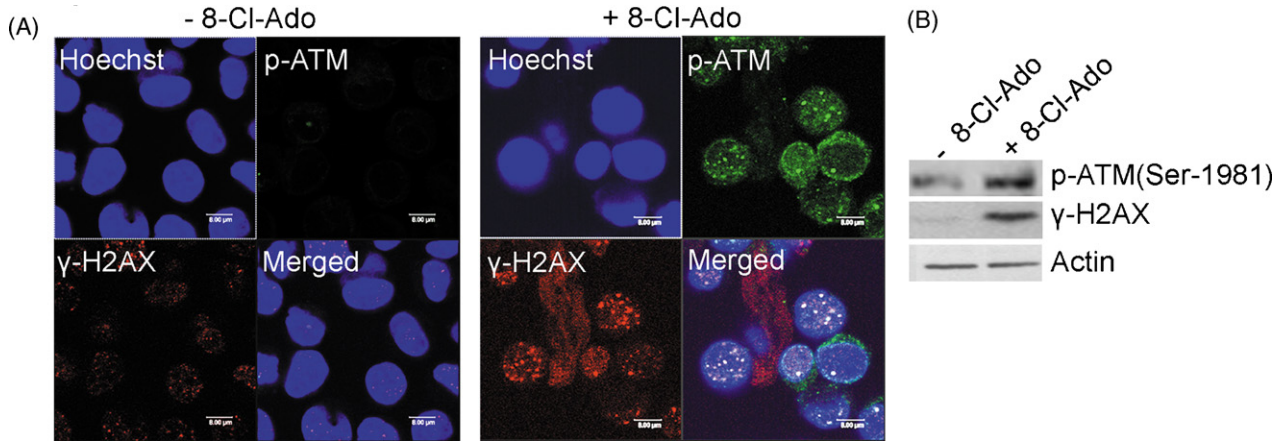

Fig. 2 – ATM-dependent γ-H2AX foci formation in exposed K562. K562 cells were unexposed or exposed to 8-Cl-Ado (10 μM) for 48 h. (A) Color co-localization of γ-H2AX with activated ATM. After cell fixation and permeabilization, the cells were immunolabeled by anti-γ-H2AX antibody or anti-phospho-ATM-S1981 antibody with Rhodamine-conjugated goat anti-rabbit IgG (for γ-H2AX) or FITC-conjugated goat anti-mouse IgG (for phospho-ATM). The nuclei were stained with Hoechst 33342 (blue). γ-H2AX was stained in red, phospho-ATM-S1981 in green. Cells were dropped on slides and viewed with Leica TCS SP2 confocal microscopy. Scale bar, 8 μm. (B) Western blotting analyses of γ-H2AX and phospho-ATM-S1981. β-Actin is used as a loading control.

Ser-139 is dependent on ATM activation in the response to 8-Cl-Ado-induced DNA DSBs in K562, immunocytochemical labeling was performed with anti-phospho-ATM-S1981 and anti-phospho-H2AX-S139 (anti-γ-H2AX) antibodies. Phosphorylated ATM and γ-H2AX could not be detected in unexposed K562. By contrast, phosphorylation of both ATM and H2AX were apparent after 8-Cl-Ado exposure, in which the patterns of immunofluorescent staining of both molecules were parallel (Fig. 2A). Consistent with the staining, phosphorylated ATM and γ-H2AX proteins were increased after exposure (Fig. 2B). These results indicate that 8-Cl-Ado exposure activates ATM kinase, which is responsible for the generation of γ-H2AX foci during DNA DSBs.

3.3. *8-Cl-Ado activates ATM-CHK1-CDC25C-CDC2 cascade in G2/M checkpoint*

To determine the cell-cycle checkpoint response to 8-Cl-Ado-induced DNA DSBs, three independent flow cytometry experiments were performed to analyze the cell-cycle distribution (Supplementary Fig. 1A). A typical flow cytometry showed that exposure of K562 cells to 8-Cl-Ado caused the increase from 16.25% to 48.26% G2/M subpopulation within 12–48 h (Fig. 3A), indicating 8-Cl-Ado-induced G2/M arrest which was similar with that of the positive control (Supplementary Fig. 1B and C) in which the K562 cells were exposed to etoposide (VP-16), a well known Topo II poison damaging DNA [30], although their mechanisms are different.

Next, we investigated the signaling pathway, responsible for G2/M checkpoint control. The phosphorylation of ATM on Ser-1981 was markedly increased in 8-Cl-Ado-exposed K562 within 12–48 h, compared with control (0 h) (Fig. 3B). To ascertain the checkpoint-transducer kinases, we examined phosphorylated substrates of ATM/ATR, the phospho-CHK2-T68 and phospho-CHK1-S345 kinases. The phospho-CHK1-S345 was substantially increased within 12–48 h after exposure. However, phospho-CHK2-T68 appeared only at a detectable level after 48 h exposure (Fig. 3C). These results indicate that CHK1 rather than CHK2 plays a dominant role in the response to 8-Cl-Ado-induced DNA DSBs. CHK kinases can phosphorylate/inactivate CDC25 phosphatases (by 14-3-3 sequestration) which activate CDK1/CDC2 kinase in G2/M checkpoint by dephosphorylation [15]. We thus examined CDC25C and CDC2. The phospho-CDC25C-S216 was increased within 12–48 h after exposure (Fig. 3D). Consistent with increased phospho-CDC25C-S216, the inactive form of CDC2 was also increased within 12–48 h (Fig. 3E). These results indicate that ATM-CHK1-CDC25C-CDC2 signal participates in the G2/M checkpoint during 8-Cl-Ado-induced DNA damage.

3.4. *BRCA1-CHK1 branch is also involved in 8-Cl-Ado-induced G2/M checkpoint*

BRCA1 can mediate activation of CHK1, which is directly responsible for G2/M arrest [31]. We analyzed the activation of BRCA1 and showed that phospho-BRCA1-S1524 was markedly increased (Fig. 4A). To determine whether BRCA1 activation is associated with the activation of CHK1 in 8-Cl-Ado-induced G2/M checkpoint, the interaction between BRCA1 and CHK1 was analyzed by coimmunoprecipitation, showing that CHK1 was present in the anti-pBRCA1 antibody-precipitated complexes (Fig. 4B). These results suggest that BRCA1-CHK1 branch is involved in 8-Cl-Ado-induced G2/M arrest.

3.5. *Inhibition of CHK1 converts G2/M checkpoint into S checkpoint*

To further illustrate the roles of CHK1 and CHK2 in 8-Cl-Ado-induced G2/M checkpoint control, the Gö6976, an inhibitor of CHK1 [25], was used in cultures. Flow cytometry showed that

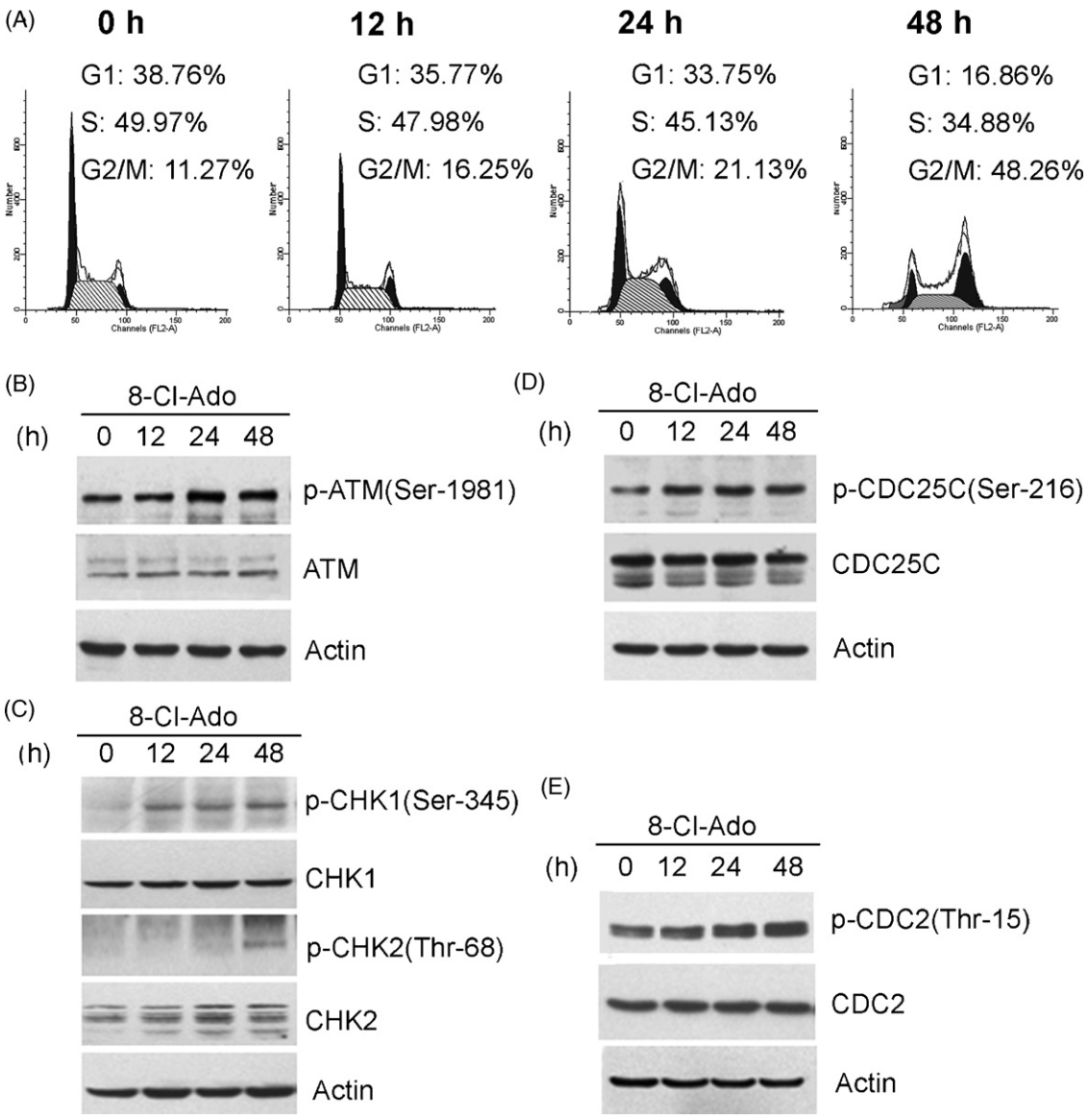

Fig. 3 – Activation of CHK1- not CHK2-related cascade in G2/M arrest by 8-Cl-Ado. K562 cells were exposed to 8-Cl-Ado (10 μM) for the indicated times. (A) Cell-cycle analysis. K562 cells were fixed with 70% ethanol and stained with propidium iodide (PI); PI signal was measured by FACScan. G1, G2/M and S populations in the cell-cycle were analyzed by computer programs. Data present one representative of three independent experiments (see Supplementary Fig. 1A). (B)–(E) Western blotting analyses of ATM, CHK1, CHK2, CDC25C, and CDC2 and their phosphorylated forms in 8-Cl-Ado-exposed K562. After the cells were extracted with lysis buffer, proteins were separated by 6–10% SDS-PAGE and transferred onto membrane, the blot was probed with specific antibodies. β-Actin as a loading control.

Gö6976 (250 nM) pretreatment plus 8-Cl-Ado exposure for 48 h caused a great decrease in G2/M population from 48.26% to 6.71%, compared with 8-Cl-Ado exposure, suggesting that Gö6976 abrogates 8-Cl-Ado-induced G2/M arrest (Fig. 5A and Supplementary Fig. 1A). Notably, Gö6976 pretreatment plus 8-Cl-Ado exposure caused 59.99% S populations which were significantly higher than that in normal culture (49.97% S populations) and in 8-Cl-Ado-exposed cells (34.88% S populations). Again, these results suggest that CHK1 but not CHK2 plays a crucial role in 8-Cl-Ado-induced G2/M checkpoint, and that inhibition of CHK1 by Gö6976 converts 8-Cl-Ado-induced G2/M checkpoint into S checkpoint.

3.6. *Gö6976 activates two parallel cascades during S checkpoint*

To understand Gö6976-converted S arrest, the S checkpoint-associated kinases and proteins were tested. Gö6976 inhibits CHK1 activity but does not affect CHK1 phosphorylation [25,26]. Supporting this finding, we found that CHK1 remained phosphorylated in the presence of Gö6976 plus 8-Cl-Ado exposure. Notably, combined treatment with Gö6976 and 8-Cl-Ado led to the significantly enhanced expression of phospho-CHK2-T68 as revealed by Western blotting (Fig. 5B). Furthermore, immunocytochemistry showed the phosphorylation

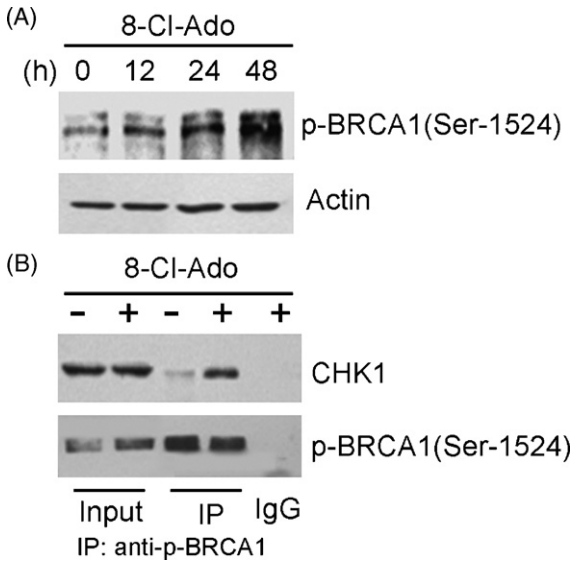

Fig. 4 – Increase of interaction between BRCA1 and CHK1 by 8-Cl-Ado. (A) Western blotting analysis of BRCA1 activation. K562 cells were exposed to 8-Cl-Ado as described in Fig. 1. BRCA1 activation was determined by Western blotting with anti-phospho-BRCA1-S1524 antibody as described in Fig. 3. β-Actin is used as a loading control. (B) Immunoprecipitation assay for BRCA1 and CHK1 interaction *in vivo*. Cells were exposed to 8-Cl-Ado for 48 h. Cell lysates were immunoprecipitated with anti-phospho-BRCA1-S1524 antibody conjugated agarose beads. Protein lysates (input), immunoprecipitated proteins by anti-phospho-BRCA1-S1524 antibody were run through 10% SDS-PAGE, transferred onto membrane and incubated with anti-CHK1 or anti-phospho-BRCA1-S1524 antibody. IgG as a negative control.

of CHK2 in the Gö6976 plus 8-Cl-Ado-treated cells and the co-localization of phospho-CHK2-T68 with phospho-ATM-S1981 in the nucleus (Fig. 6). However, the co-localization of phospho-CHK1-S345 with phospho-ATM-S1981 was failed to be detected (data not shown). These results suggest a displacement of CHK1 function by CHK2 in the presence of Gö6976. In response to DNA damage, the degradation of CHK2-phosphorylated CDC25A results in S-phase arrest [32]. Thus, we examined CDC25A which was decreased in total in 8-Cl-Ado/Gö6976-treated K562 (Fig. 5C). Consistent with the reduction of CDC25A phosphatase, the levels of phosphorylated CDK2 were not changed (Fig. 5C).

Because activated NBS1 [20,33] and SMC1 [21,22] by ATM play roles in S-phase checkpoint, the activated forms of the two molecules were determined (Fig. 5D). Western blotting showed that the phosphorylation of NBS1 on Ser-343 and SMC1 on Ser-957 was markedly increased in 8-Cl-Ado/Gö6976-treated K562.

Together, these results in Fig. 5 indicate that two parallel branches, the ATM-CHK2-CDC25A-CDK2 and the ATM-NBS1/SMC1 pathways participate in Gö6976-converted S-phase checkpoint.

3.7. *Inhibition of CHK1 enhances 8-Cl-Ado-induced DNA damage*

To explore the biological meaning of the conversion of G2/M checkpoint into S checkpoint by Gö6976, γ-H2AX nuclear foci were examined. Immunocytochemistry showed that exposure of K562 cells to 8-Cl-Ado with Gö6976 pretreatment increased the numbers of γ-H2AX foci (Fig. 7A), compared with exposure to 8-Cl-Ado alone. Increased γ-H2AX protein and poly(ADP-ribose) polymerase-1 (PARP-1) activation were also detected by Western blotting (Fig. 7B). These results suggest that the inhibition of CHK1 by Gö6976 promotes 8-Cl-Ado-induced DNA damage.

3.8. *Gö6976-converted S checkpoint inhibits replication-origin firing*

Activation of S-phase checkpoint will inhibit the firing from the origins of DNA replication that have not yet been initiated, to which CDC45 is required and inhibition of CDK2 activity blocks the loading of CDC45 onto DNA [34]. Thus, we observed CDC45 loading onto DNA using immunocytochemistry. The decrease of CDC45 localization on the nucleus (DNA) was greatly expanded by 8-Cl-Ado/Gö6976 (Fig. 8A right-lower). By contrast, the p21 located in the nucleus was increased. The decrease of CDC45 loading onto DNA suggests that Gö6976-converted S-phase checkpoint inhibits the replication-origin firing in the cells. To explore the mechanism of decreased CDC45 loading onto DNA, CDC45 and p21 were determined. Western blotting showed that 8-Cl-Ado plus Gö6976 (250 nM) up-regulated p21 markedly, but did not affect the levels of CDC45 significantly (Fig. 8B). These results suggest that the decrease of CDC45 loading onto DNA is attributed to the up-regulation of p21 which participates in CHK2-CDC25A cascade-mediated CDK2 inhibition [34].

4. Discussion

The mechanisms of 8-Cl-cAMP and 8-Cl-Ado actions are complicated, which involve several biological processes including cell-cycle arrest [3,4,9,27,28], apoptosis [3–8,10,27], mitotic catastrophe [27], differentiation [1,2,5], and chromosome breaks [13]. Although protein kinase A-regulated differentiation [1], protein kinase C-linked growth inhibition [9], and p38 MAP kinase-mediated apoptosis [10] in the response to 8-Cl-cAMP or 8-Cl-Ado have been documented, the cell-cycle checkpoint pathways need to be studied. Supporting the observation of chromosome cleavage [13], we have recently shown that 8-Cl-Ado exposure can damage DNA in cancer cells through inhibiting topoisomerase II by 8-Cl-Ado-converted 8-Cl-ATP [14]. In this study, we demonstrate that 8-Cl-Ado-induced DNA damage activates G2/M phase checkpoint in human leukemia K562 cells, which is associated with ATM-activated CHK1-CDC25C-CDC2 cascade joined by BRCA1-CHK1. Inhibition of CHK1 kinase by Gö6976 can promote DNA damage and activate CHK2, converting G2/M checkpoint into intra-S-phase checkpoint in which two parallel branches, the ATM-CHK2-CDC25A-CDK2 and the ATM-NBS1/SMC1 cascades are involved. These observations

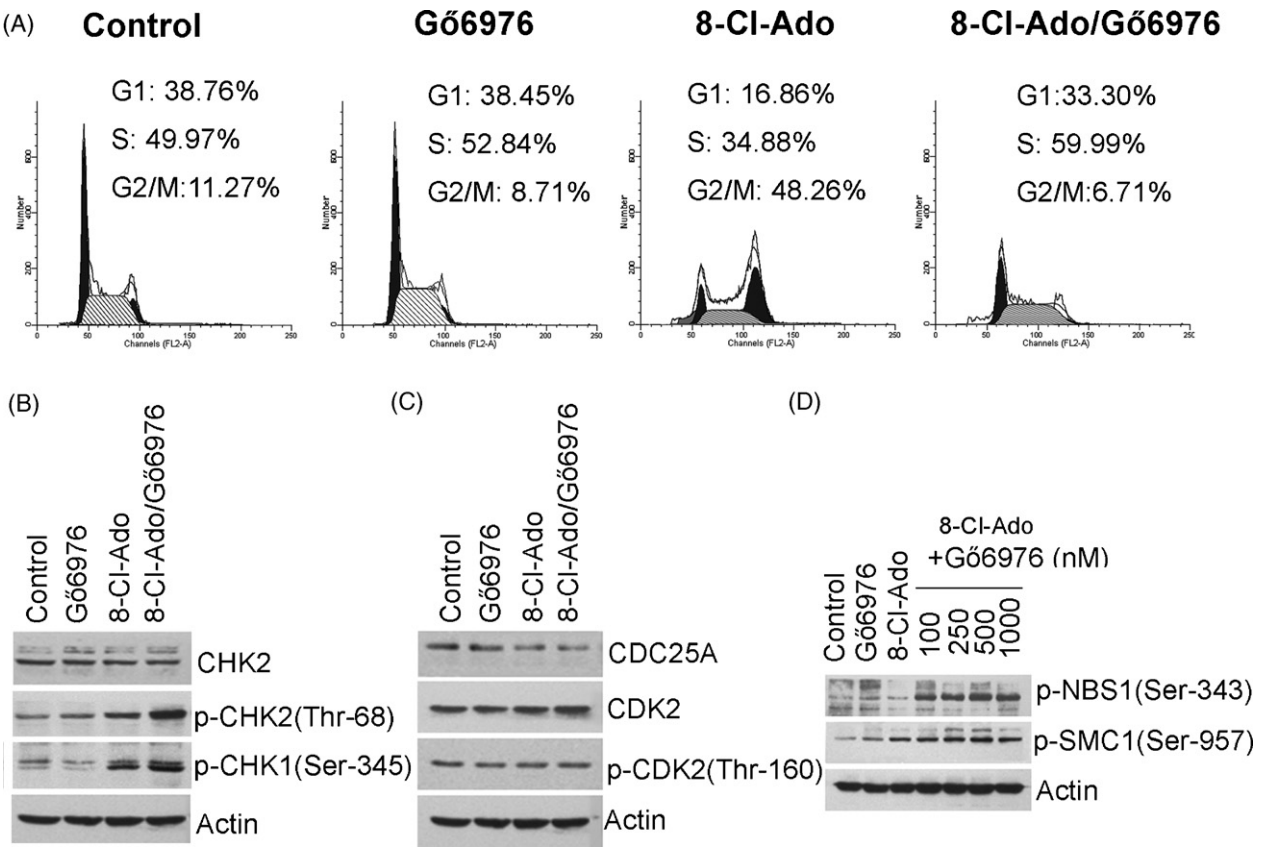

Fig. 5 – Activation of CHK2 and related proteins in Gö6976-converted S checkpoint. K562 cells were exposed to 8-Cl-Ado (10 μM) for 48 h in the presence or absence of Gö6976 (250 nM). (A) Cell-cycle analysis. The cells were stained with propidium iodide (PI) and PI signals were measured by FACScan as described in Fig. 3A. Data present one representative of three independent experiments (see Supplementary Fig. 1A). (B) and (C) Western blotting analyses of CHK1, CHK2, CDC25A, and CDK2 in 8-Cl-Ado/Gö6976-exposed K562. After the cellular proteins were separated and transferred onto membrane, the blot was probed with specific antibodies. (D) Analyses of NBS1 and SMC1 activation. K562 was treated for 48 h by 8-Cl-Ado and Gö6976 as indicated on the top. Western blotting was performed with specific antibodies. β-Actin as a loading control.

may provide aid in better understanding of the mechanisms of 8-Cl-cAMP and 8-Cl-Ado actions and in potential design of the combined therapy.

This is not the case of human lung cancer A549 and H1299 cell lines, in which 8-Cl-Ado exposure leads to loss of inhibitory phosphorylation of CDC2 and CDC25C, which allows progression into mitosis, followed by aberrant mitosis and failed cytokinesis [27]. Although there is ATM activation in exposed A549 and H1299, it is not so exciting (unpublished). The difference between A549 and K562 in the response to the agent may implicate different sensitivities to the agent. This is reminiscent of the variety of 8-Cl-cAMP- and 8-Cl-Ado-induced growth inhibition by apoptosis [3–8,10], mitotic catastrophe [27] and differentiation [1,2,5], which is possibly attributable to the elements such as the cell-types, lesion degrees and properties, administration dosages, environments, even the methods involved in the studies, affecting the cellular responses to the agent.

In normal cells, p53 tumor suppressor exerts a pivotal role in controlling the cell-cycle, apoptosis, and DNA repair in response to various forms of genotoxic stress [15]. Since p53 is mutated in approximately 50% of human cancers, other checkpoint regulators should be involved in regulating the cellular response to genotoxic stress. The key transcriptional target of p53 is the p21Waf1/Cip1 inhibitor of cyclin-dependent kinase [35], which silences the G1/S-promoting Cyclin E/CDK2 kinase and thereby causes a G1 arrest. The loss of p53 function abrogates the G1 checkpoint and may compromise a G2 checkpoint pathway that operates in parallel with those governed by ATR and/or ATM. In this study we found that in p53-null K562, 8-Cl-Ado-induced DNA damage activated G2/M phase checkpoint control which was associated with ATM-activated CHK1-CDC25C-CDC2 cascade joined by BRCA1-CHK1 branch (Figs. 3 and 4). In the cross-talk between these pathways, CHK1 seems to be a key regulator (Fig. 9). It is generally believed that the agents interfering with related proteins in specific checkpoint pathways may preferentially sensitize cancer cells to chemotherapy- and radiation-induced killing. We therefore determined the signaling pathways involved in DNA-damage response in p53-null K562 and found that the potent inhibition of CHK1 kinase activity by Gö6976 could promote 8-Cl-Ado-induced DNA damage in p53-

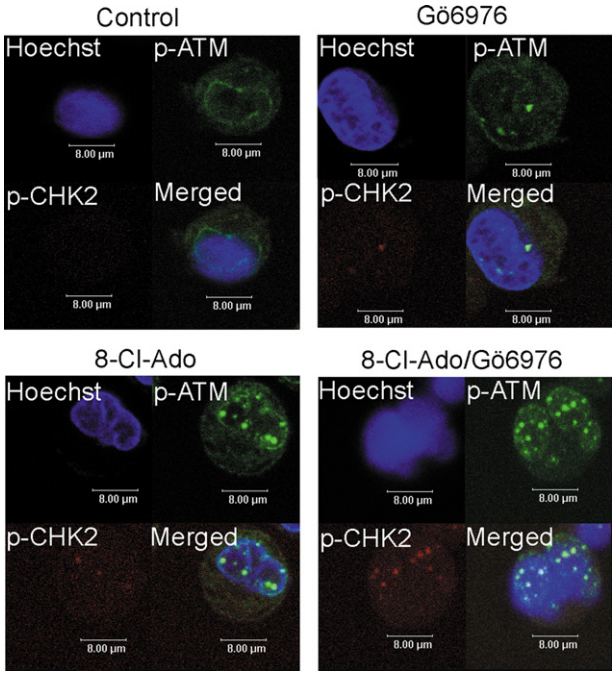

Fig. 6 – ATM-dependent CHK2 activation in 8-Cl-Ado/Gö6976-treated K562. K562 cells were exposed to 8-Cl-Ado (10 μM) for 48 h in the presence or absence of Gö6976 (250 nM). After fixation and permeabilization, the cells were immunolabeled by anti-phospho-CHK2-T68 and anti-phospho-ATM-S1981 antibodies with Rhodamine-conjugated goat anti-rabbit IgG (for phospho-CHK2) or FITC-conjugated goat anti-mouse IgG (for phospho-ATM). The nuclei were stained with Hoechst 33342 (blue), phospho-CHK2-T68 stained in red, phospho-ATM-S1981 in green. Cells were dropped on slides and viewed with Leica TCS SP2 confocal microscopy. Scale bar, 8 μm.

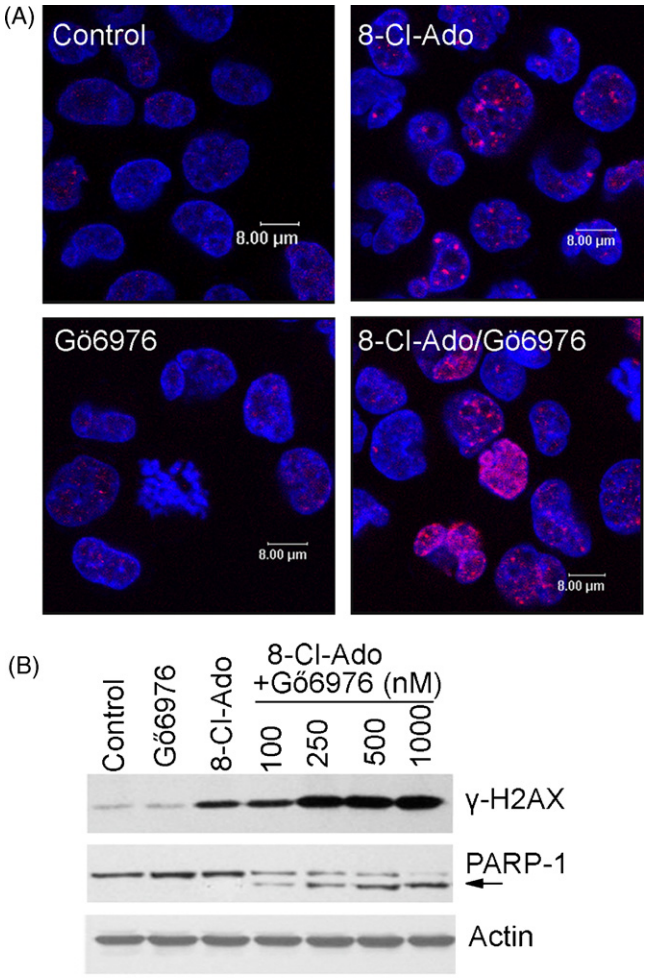

Fig. 7 – Promotion of 8-Cl-Ado-induced DNA breaks by Gö6976. K562 cells were exposed to 8-Cl-Ado (10 μM) for 48 h in the presence or absence of Gö6976 (250 nM). (A) Immunocytochemistry for γ-H2AX nuclear foci. After harvested, the cells were immunolabeled with anti-γ-H2AX antibody and Rhodamine-conjugated goat anti-rabbit IgG (red). The nuclei were stained with Hoechst 33342 (blue). Cells were dropped on slides and viewed with Leica TCS SP2 confocal microscopy. Scale bar, 8 μm. (B) Analyses of γ-H2AX and PARP-1 activation. K562 was treated for 48 h by 8-Cl-Ado and Gö6976 as indicated on the top. Western blotting was performed with specific antibodies. β-Actin as a loading control.

deficient cells (Fig. 7), followed by increased apoptosis (data not shown). These results may provide evidence for searching rationalized approaches to treat p53-deficient cancer.

ATM and ATR are first activated by autophosphorylation in response to DNA damage [15–18]. We observed the increases of phospho-ATM-S1981 and ATM-phosphorylated histone H2AX on Ser-139 (Figs. 1 and 2), suggesting involvement of ATM in the response to 8-Cl-Ado-induced DNA damage. Usually, ATM phosphorylates CHK2 on Thr-68 leading to CHK2 activation [36,37], and ATR activates CHK1. However, both ATM and ATR may phosphorylate CHK1 on Ser-317 and Ser-345 [15,34]. We found that phospho-CHK1-S345 was substantially increased after 8-Cl-Ado exposure, which was parallel with the ATM activation, whereas phospho-CHK2-T68 appeared only at a detectable level after 48 h exposure (Fig. 3C). We therefore suggest that CHK1 plays a dominant role in the response to 8-Cl-Ado-induced DNA damage. The role of CHK1 in 8-Cl-Ado-induced G2/M checkpoint can also be drawn from the conversion of G2/M into S arrest by the inhibitor of CHK1, Gö6976 (Fig. 5A and Supplementary Fig. 1A). BRCA1, as an ATM substrate, mediates multi-protein interactions, facilitating ATM signaling and the processing/repairing of the lesions [38,39]. Also, BRCA1 controls the expression, phosphorylation and cellular localization of CDC25C and CDC2 kinase through activating CHK1 by BRCA1 [31]. We did find the increased BRCA1 activation (phospho-BRCA1-S1524) (Fig. 4A) and its interaction with CHK1 in exposed K562 (Fig. 4B). Thus, the CHK1 can be activated by both ATM and BRCA1 in exposed cells, which is correlated to the inhibitory phosphorylation of CDC25C and CDC2/CDK1 (Fig. 3D and E). We conclude that BRCA1-CHK1 branch participates in ATM-CHK1-CDC25C-CDC2 mediated G2/M checkpoint (Fig. 9).

The involvement of CHK1 in G2/M checkpoint might imply an unique mechanism of 8-Cl-Ado-induced DNA damage.

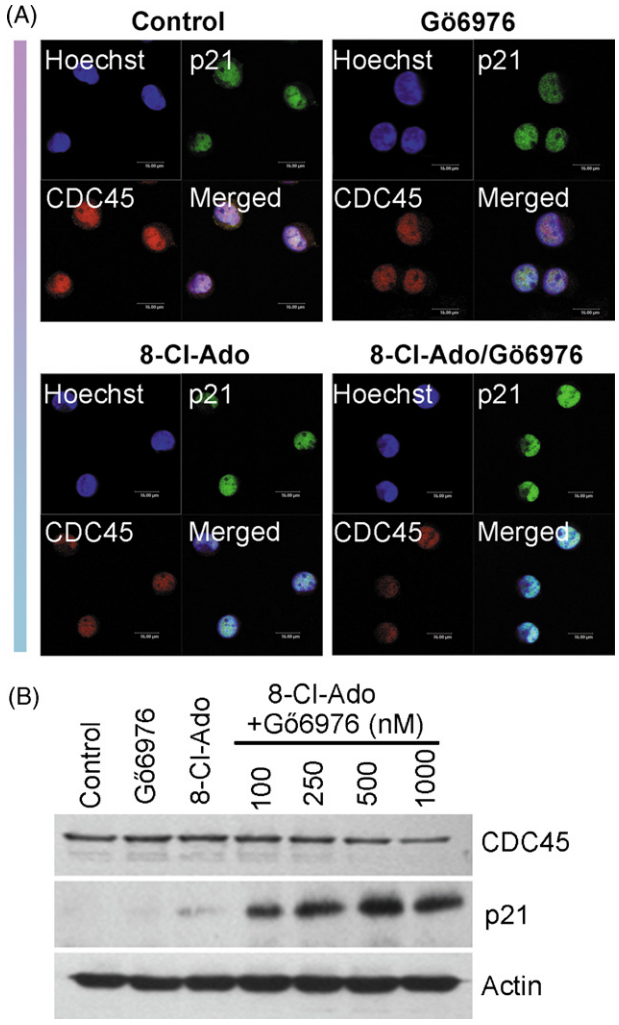

Fig. 8 – Increased inhibition of CDC45 loading onto DNA by Gö6976. K562 cells were exposed to 8-Cl-Ado (10 μM) for 48 h in the presence or absence of Gö6976 (250 nM). (A) Immunocytochemical analysis of CDC45 loading onto nuclear DNA. The cells were immunolabeled with anti-CDC45 and anti-p21 antibodies and Rhodamine-conjugated goat anti-rabbit (for CDC45) or FITC-conjugated goat anti-mouse IgG (for p21). CDC45 was stained in red, p21 in green, and nuclei were stained with Hoechst 33342 in blue. Cells were dropped on slides and viewed with Leica TCS SP2 confocal microscopy. Scale bar, 16 μm. The color box on the left shows relative fluorescence intensity. (B) Analyses of CDC45 and p21. K562 was treated for 48 h by 8-Cl-Ado and Gö6976 as indicated on the top. Western blotting was performed with specific antibodies. β-Actin as a loading control.

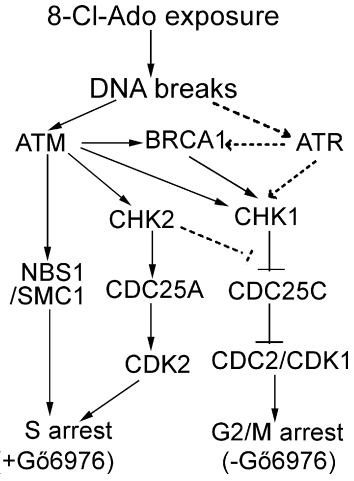

Fig. 9 – Schematic diagram showing cell-cycle checkpoint pathways induced in the response to 8-Cl-Ado-induced DNA damage in the presence and absence of Gö6976. Dotted lines refer to unidentified events.

ATM-CHK2 is primarily activated following DNA damage, while ATR-CHK1 is critical for cellular responses to the arrest of DNA replication forks [15–17] that is processed to DSBs and recombination [19,20,40,41]. 8-Cl-Ado can be converted into 8-Cl-ATP in cells [8]. Recently, we demonstrated that 8-Cl-ATP, as an ATP analog, could inhibit ATP-dependent topoisomerase II activities in cells [14]. The unique decatenating and unknotting activity of Topo II is essential to efficiently carry out segregation of daughter chromosomes after DNA replication. We therefore suppose that lacking Topo II-mediated decatenation, cells try to segregate intertwined sister chromatids during mitosis, then chromosome breakage may occur, as previous observation [13]. Furthermore, 8-Cl-ATP as a "true" Topo II catalytic inhibitor (not poison) can increase closed-clamp stability [14], interfering with the progression of the replication fork. In addition, 8-Cl-ATP inhibits RNA synthesis [11,12]. Because RNA primers are required for the synthesis of lagging strand, the lagging strand synthesis might be slowed-down during 8-Cl-Ado exposure, resulting in uncoupling of leading and lagging strand replication, which is similar to stalled replication forks. The complicated mechanisms of DNA damage lead to the activation of CHK1 that joins two parallel branches, the CHK1-CDC25C-CDC2 and BRCA1-CHK1 cascades. Considering replication fork arrest, we do not exclude the possibility of the ATR activation at the earlier stage of 8-Cl-Ado exposure (Fig. 9).

ATM-activated CHK2 can phosphorylate p53 [42], CDC25A [32], and CDC25C [36,37], contributing to the G1/S, S, and G2/M checkpoints, respectively. A recent study shows that CHK2 participates in S-phase checkpoint in the response to irofulven-induced DNA damage [43]. It is also demonstrated that in response to ionizing radiation, the phosphorylation of CHK2 and NBS1 by ATM triggers two parallel branches of the DNA damage-dependent S-phase checkpoint, the ATM-CHK2-CDC25A-CDK2 and ATM-NBS1/MRE11 cascades, to delay DNA replication [32]. In addition, it is shown that two or more pathways act in concert to cause S-phase arrest after ionizing irradiation, in which phosphorylation of SMC1 on Ser-957 and Ser-966 is involved [21,38]. In this work, we found that pretreatment with Gö6976 stimulated the phosphorylations of CHK2 on Thr-68 (Fig. 5B and Fig. 6), NBS1 on Ser-343, and SMC1 on Ser-957 (Fig. 5D) in 8-Cl-Ado-exposed K562, converting G2/M checkpoint into intra-S-phase checkpoint (Fig. 5A and Supplementary Fig. 1A). Although we did not test CDC25A

phosphorylation, the decrease of CDC25A phosphatase was observed, which should be attributable to CHK2-mediated CDC25A-degradation cascade. The maintenance of inhibitory phosphorylation of CDK2 was also detected (Fig. 5C). Therefore we suggest that two parallel branches, the ATM-CHK2-CDC25A-CDK2 and the ATM-NBS1/SMC1 pathways, participate in Gö6976-converted S-phase checkpoint (Fig. 9).

Mammalian cells exposed to ionizing radiation activate ATM, which initiates complex responses including the S-phase checkpoint pathway to delay DNA replication [32,44]. Loading of CDC45 onto DNA, which is required for recruiting DNA polymerase α into assembled pre-initiation complexes at the origins of DNA, requires the activity of CDK2 [32,45]. Inhibition of CDK2 may prevent the initiation of new origin firing [34]. We observed the reduction of CDC45 loading onto DNA in 8-Cl-Ado/Gö6976 combined exposed K562 (Fig. 8A). Because CDC45 abundance had little changed (Fig. 8B), the reduction of CDC45 loading must be attributable to the inhibition of CDK2 by inhibitory phosphorylation through CHK2-CDC25A-degradation cascade. In addition, we observed the up-regulation of p21 in 8-Cl-Ado/Gö6976 exposed cells (Fig. 8B), which may also contribute to the inhibition of CDK2.

It is reported that Gö6976 inhibits CHK1 and perhaps CHK2 kinase activity but does not decrease their phosphorylation [25]. Later study shows that Gö6976 inhibits CHK1 but not CHK2 activity [26]. The agent is very effective to sensitize cells to DNA damage through abrogation of the S and G2 arrest [25,26]. Differently, we found that Gö6976-converted 8-Cl-Ado-iduced G2/M checkpoint into S checkpoint (Fig. 5A and Supplementary Fig. 1A). This might be due to different doses of Gö6976, treatment way and cell-types. For instance, Gö6976 can potently abrogate S and G2 arrest and enhance the cytotoxicity of the topoisomerase I inhibitor SN38 only in p53-defective MDA-MB-231 cells, but has not effect in the wild-type p53 MCF-10a cells [25]. A dose–effect analysis shows that 30 nM Gö6976 is sufficient to cause abrogation of S and G2 arrest in breast cancer MDA-MB-231 cells [25]. In our study, however, no significant effect could be seen with Gö6976 at a concentration of lower than 100 nM in human chronic myelocytic leukemia K562 cells. In HeLa cells stimulated by HU, an effective dose of Gö6976 to inhibit CHK1 activity was 600 nM [26]. In addition, the culture conditions (e.g., the variety of medium and the presence of insulin and epidermal growth factor [25]) may affect the effectiveness of the agent.

We found that Gö6976 enhanced 8-Cl-Ado-induced DNA damage in concentration-dependent manner (Fig. 7). It is possible that abrogation of G2 (or G2/M) phase checkpoint drives cells through mitosis, where cells force a segregating of intertwined sister chromatids, resulting in increased DNA breaks, under the condition of 8-Cl-ATP-inhibited topoisomerase II. It is also possible that increased DNA damage results from the activation of PARP-1 which is a target for PKC [46] and often induced by DNA breaks [47]. The phosphorylation of PARP-1 by PKC inhibits its activation [48]. Therefore it is plausible to assume that inhibition of PKC by Gö6976 may increase PARP-1 activation (Fig. 7B). PARP-1 activation consumes NAD^+, resulting in ATP depletion, which, in turn, inhibits DNA repair [47] and may strengthen the inhibition of ATP-dependent topoisomerase II by 8-Cl-ATP, thereby increasing DNA breaks and cell death. Our data can explain the previous observation that adding PKC inhibitors cannot turn back the end, although activation of PKC inhibits cell growth [9].

In summary, 8-Cl-Ado exposure activates ATM-CHK1-CDC25C-CDC2 pathway joined by BRCA1-CHK1 branch in the response to 8-Cl-Ado-induced DNA damage, which is correlated to G2/M phase checkpoint. Inhibition of CHK1 by Gö6976 promotes DNA damage and leads to the activation of CHK2, converting G2/M checkpoint into intra-S-phase checkpoint in which both the ATM-NBS1/SMC1 and the ATM-CHK2-CD25A-Cyclin E/CDK2 branches are involved. These data suggest that the combination of CHK1 inhibitor Gö6976 with 8-Cl-Ado may be a potentially clinical therapeutics.

Acknowledgements

This work was funded by National Natural Science Foundation of PR China grants 30471975, 30671062, 30621002 and Education Committee of Beijing Teaching Reinforcing Plan.

Appendix A. Supplementary data

Supplementary data associated with this article can be found, in the online version, at doi:10.1016/j.bcp.2008.11.008.

REFERENCES

[1] Rohlff C, Clair T, Cho-Chung YS. 8-Cl-cAMP induces truncation and down-regulation of the RI alpha subunit and up-regulation of the RII beta subunit of cAMP-dependent protein kinase leading to type II holoenzyme-dependent growth inhibition and differentiation of HL-60 leukemia cells. J Biol Chem 1993;268:5774–82.
[2] Tortora G, Pepe S, Yokozaki H, Meissner S, Cho-Chung YS. Cooperative effect of 8-Cl-cAMP and rhGM-CSF on the differentiation of HL-60 human leukemia cells. Biochem Biophys Res Commun 1991;177:1133–40.
[3] Grbovic O, Jovic V, Ruzdijic S, Pejanovic V, Rakic L, Kanazir S. 8-Cl-cAMP affects glioma cell-cycle kinetics and selectively induces apoptosis. Cancer Invest 2000;20:972–82.
[4] Kim SN, Ahn YH, Kim SG, Park SD, Cho-Chung YS, Hong SH. 8-Cl-cAMP induces cell cycle-specific apoptosis in human cancer cells. Int J Cancer 2001;93:33–41.
[5] Fassina G, Aluigi MG, Gentleman S, Wong P, Cai T, Albini A, et al. The cAMP analog 8-Cl-cAMP inhibits growth and induces differentiation and apoptosis in retinoblastoma cells. Int J Cancer 1997;72:1088–94.
[6] Halgren RG, Traynor AE, Pillay S, Zell JL, Heller KF, Krett NL, et al. 8-Cl-cAMP cytotoxicity in both steroid sensitive and insensitive multiple myeloma cell lines is mediated by 8-Cl-adenosine. Blood 1998;92:2893–8.
[7] Carlson CC, Chinery R, Burnham LL, Dransfield DT. 8-Cl-adenosine-induced inhibition of colorectal cancer growth in vitro and in vivo. Neoplasia 2000;2:441–8.
[8] Gandhi V, Ayres M, Halgren RG, Krett NL, Newman RA, Rosen ST. 8-chloro-cAMP and 8-chloro-adenosine act by the same mechanism in multiple myeloma cells. Cancer Res 2001;61:5474–9.
[9] Ahn YH, Jung JM, Hong SH. 8-Cl-cAMP and its metabolite, 8-Cl-adenosine induce growth inhibition in mouse fibroblast

DT cells through the same pathways; protein kinase C activation and cyclin B downregulation. J Cell Physiol 2004;201:277–85.
[10] Ahn YH, Jung JM, Hong SH. 8-Chloro-cyclic AMP-induced growth inhibition and apoptosis is mediated by p38 mitogen-activated protein kinase activation in HL60 cells. Cancer Res 2005;65:4896–901.
[11] Stellrecht CM, Rodriguez Jr CO, Ayres M, Gandhi V. RNA directed actions of 8-chloro-adenosine in multiple myeloma cells. Cancer Res 2003;63:7968–74.
[12] Chen LS, Sheppard TL. Chain termination and inhibition of *Saccharomyces cerevisiae* poly(A) polymerase by C-8-modified ATP analogs. J Biol Chem 2004;279:40405–11.
[13] Bajic A, Stanimirovic Z, Stevanovic J. Genotoxicity potential of 8-Cl-cyclic adenosine monophosphate assessed with cytogenetic tests in vivo. Arch Med Res 2004;35:209–14.
[14] Yang S-Y, Jia X-Z, Feng L-Y, Li S-Y, An G-S, Ni J-H, et al. Inhibition of topoisomerase II by 8-chloro-adenosine triphosphate induces DNA double-stranded breaks in 8-chloro-adenosine-exposed human myelocytic leukemia K562 cells. Biochem Pharmacol 2009;77:433–43.
[15] Kastan MB, Bartek J. Cell-cycle checkpoints and cancer. Nature 2004;432:316–23.
[16] Shiloh Y. ATM and related protein kinases: safeguarding genome integrity. Nat Rev Cancer 2003;3:155–68.
[17] Liu QH, Guntuku S, Cui XS, Matsuoka S, Cortez D, Tamai K, et al. Chk1 is an essential kinase that is regulated by ATR and required for the G2/M DNA damage checkpoint. Genes Dev 2000;14:1448–59.
[18] Rogakou EP, Boon C, Redon C, Bonner WM. Megabase chromatin domains involved in DNA double-strand breaks in vivo. J Cell Biol 1999;146:905–15.
[19] Thiriet C, Hayes JJ. Chromatin in need of a fix: phosphorylation of H2AX connects chromatin to DNA repair. Mol Cell 2005;18:617–22.
[20] Lim DS, Kim ST, Xu B, Maser RS, Lin JY, Petrini JHJ, et al. ATM phosphorylates p95/nbs1 in an S-phase checkpoint pathway. Nature 2000;404:613–7.
[21] Kim ST, Xu B, Kastan MB. Involvement of the cohesin protein, Smc1, in Atm-dependent and independent responses to DNA damage. Genes Dev 2002;16:560–70.
[22] Yazdi PT, Wang Y, Zhao S, Patel N, Lee EY-HP, Qin J. SMC1 is a downstream effector in the ATM/NBS1 branch of the human S-phase checkpoint. Genes Dev 2002;16:571–82.
[23] Xu B, Kim ST, Kastan MB. Involvement of Brca1 in S-phase and G_2-phase checkpoints after ionizing irradiation. Mol Cell Biol 2001;21:3445–50.
[24] Kawabe T. G2 checkpoint abrogation as a cancer specific, cell cycle disruption. Ann Cancer Res Ther 2005;13:17–22.
[25] Kohn EA, Yoo CJ, Eastman A. The protein kinase C inhibitor Gö6976 is a potent inhibitor of DNA damage-induced S and G2 cell cycle checkpoints. Cancer Res 2003;63:31–5.
[26] Ishimi Y, Komamura-Kohno Y, Kwon HJ, Yamada K, Nakanishi M. Identification of MCM4 as a target of the DNA replication block checkpoint system. J Biol Chem 2003;278:24644–50.
[27] Zhang H-Y, Gu Y-Y, Li Z-G, Jia Y-H, Yuan L, Li S-Y, et al. Exposure of human lung cancer cells to 8-chloro-adenosine induces G2/M arrest and mitotic catastrophe. Neoplasia 2004;6:802–12.
[28] Gu Y-Y, Zhang H-Y, Zhang H-J, Li S-Y, Ni J-H, Jia H-T. 8-Chloro-adenosine inhibits growth at least partly by interfering with actin polymerization in cultured human lung cancer cells. Biochem Pharmacol 2006;72:541–50.
[29] Huang X, Okafuji M, Traganos F, Luther E, Holden E, Darzynkiewicz Z. Assessment of histone H2AX phosphorylation induced by DNA topoisomerase I and II inhibitors topotecan and mitoxantrone and by the DNA cross-linking agent cisplatin. Cytometry A 2004;58:99–110.
[30] Liu LF. DNA topoisomerase poisons as antitumor drugs. Annu Rev Biochem 1989;58:351–75.
[31] Yarden RI, Pardo-Reoyo S, Sgagias M, Cowan KH, Brody LC. BRCA1 regulates the G2/M checkpoint by activating Chk1 kinase upon DNA damage. Nat Genet 2002;30:285–9.
[32] Falck J, Petrini JHJ, Williams BR, Lukas J, Bartek J. The DNA damage-dependent intra-S phase checkpoint is regulated by parallel pathways. Nat Genet 2002;30:290–4.
[33] Buscemi G, Savio C, Zannini L, Miccichè F, Masnada D, Nakanishi M, et al. Chk2 activation dependence on Nbs1 after DNA damage. Mol Cell Biol 2001;21:5214–22.
[34] Bartek J, Lukas J. Chk1 and Chk2 kinases in checkpoint control and cancer. Cancer Cell 2003;3:421–9.
[35] Kastan MB, Lim DS. The many substrates and functions of ATM. Mol Cell Biol 2000;1:179–86.
[36] Matsuoka S, Huang M, Elledge SJ. Linkage of ATM to cell cycle regulation by the Chk2 protein kinase. Science 1998;282:1893–7.
[37] Chaturvedi P, Eng WK, Zhu Y, Mattern MR, Mishra R, Hurle MR, et al. Mammalian Chk2 is a downstream effector of the ATM-dependent DNA damage checkpoint pathway. Oncogene 1999;18:4047–54.
[38] Kitagawa R, Bakkenist CJ, McKinnon PJ, Kastan MB. Phosphorylation of SMC1 is a critical downstream event in the ATM-NBS1-BRCA1 pathway. Genes Dev 2004;18:1423–38.
[39] Wiltshire T, Senft J, Wang Y, Konat GW, Wenger SL, Reed E, et al. BRCA1 contributes to cell cycle arrest and chemoresistance in response to the anticancer agent irofulven. Mol Pharmacol 2007;71:1051–60.
[40] Michel B, Ehrlich SD, Uzest M. DNA double-strand breaks caused by replication arrest. Eur Mol Biol Org J 1997;16:430–8.
[41] Cortés-Ledesma F, Aguilera A. Double-strand breaks arising by replication through a nick are repaired by cohesin-dependent sister-chromatid exchange. Eur Mol Biol Org Rep 2006;7:919–26.
[42] Hirao A, Kong YY, Matsuoka S, Wakeham A, Ruland J, Yoshida H, et al. DNA damage-induced activation of p53 by the checkpoint kinase Chk2. Science 2000;287:1824–7.
[43] Wang J, Wiltshire T, Wang Y, Mikell C, Burks J, Cunningham C, et al. ATM-dependent CHK2 activation induced by anticancer agent, Irofulven. J Biol Chem 2004;279:39584–92.
[44] Rotman G, Shiloh Y. ATM: a mediator of multiple responses to genotoxic stress. Oncogene 1999;18:6135–44.
[45] Zou L, Stillman B. Assembly of a complex containing Cdc45p, replication protein A, and Mcm2p at replication origins controlled by S-phase cyclin dependent kinases and Cdc7p-Dbf4p kinase. Mol Cell Biol 2000;20:3086–96.
[46] Tanaka Y, Koide SS, Yoshihara K, Kamiya T. Poly(ADP-ribose) synthetase is phosphorylated by protein kinase C in vitro. Biochem Biophys Res Commun 1987;148:709–17.
[47] Bentle MS, Reinicke KE, Bey EA, Spitz DR, Boothman DA. Calcium-dependent modulation of poly(ADP-ribose) polymerase-1 alters cellular metabolism and DNA repair. J Biol Chem 2006;281:33684–96.
[48] Bauer PI, Farkas G, Buday L, Mikala G, Meszaros G, Kun E, et al. Inhibition of DNA binding by the phosphorylation of poly ADP-ribose polymerase protein catalysed by protein kinase C. Biochem Biophys Res Commun 1992;187:730–6.